Available online at www.CivileJournal.org

Civil Engineering Journal

(E-ISSN: 2476-3055; ISSN: 2676-6957)

Vol. 10, No. 06, June, 2024

M-N Interaction Diagrams of RC Columns Strengthened with Steel C-Sections and Battens

Hamza M. Salman [1*], Mohannad H. Al-Sherrawi [1]

[1] *Department of Civil Engineering, College of Engineering, University of Baghdad, Baghdad, Iraq.*

Received 04 February 2024; Revised 29 April 2024; Accepted 08 May 2024; Published 01 June 2024

Abstract

Due to design errors and changes in the use of buildings, reinforced concrete (RC) columns must often be strengthened to support additional live loads. The column must be designed to withstand both axial loads and bending moments, and an interaction diagram is necessary to demonstrate the column failure. The most common technique for strengthening RC columns uses a steel jacket consisting of four steel angles and battens. In this study, another strengthening technique was proposed that uses two steel C-sections with steel battens. A new approach for constructing an axial force-bending moment interaction diagram for RC columns strengthened with steel C-section jackets using an analytical model based on the plastic stress distribution method was introduced. A finite element (FE) model was created using Abaqus software, and the FE results were consistent with the experimental and analytical results. The analytical and FE results showed that this strengthening method was effective and increased the axial load and bending moment capacities of the strengthened columns. This increase was explained by the confining effect of the steel jacket and the ability of the steel C-sections to withstand a large part of the applied load. This approach offers an effective and economical solution for the reinforcement of RC columns and provides a reliable and safe option for structural engineers.

Keywords: C-Section; Finite Element Model; M-N Interaction Diagram; Reinforced Concrete Column; Steel Jacket.

1. Introduction

Columns are the main load-carrying structural elements in framed buildings and are vulnerable to frame aging and design deficiencies during their construction. The structural performance of columns can be retrofitted and enhanced by strengthening them to satisfy the latest safety requirements in terms of the required load-carrying capacity, ductility, and stiffness. A popular method for strengthening reinforced concrete (RC) columns includes the use of steel jackets [1]. The steel jacket technique is commonly used to strengthen and improve the deformation capacity of RC columns in existing buildings, and presents critical conditions for seismic and gravity loads [2, 3].

The interaction diagram of a column cross-section can be used to determine its load-bearing capacity. This diagram shows the correlation between the ultimate axial load capacity and the bending moment capacity of a given column cross section. By referring to this curve, it is easy to determine whether a section is safe. However, it is difficult to obtain information regarding the development of an interaction diagram for an RC rectangular column reinforced with a steel jacket. Experimental tests were conducted to formulate an interaction diagram for RC rectangular columns strengthened with steel angles or composite sections. The plastic stress distribution method (PSDM) is one of the methods used to create an M-N interaction diagram for a composite RC column. The method developed is simple and applicable in the practical design field [4–7].

* Corresponding author: hamza.m@coeng.uobaghdad.edu.iq

http://dx.doi.org/10.28991/CEJ-2024-010-06-016

In this study, the effect of strengthening RC columns with a steel jacket on the axial load and bending moment capacities was investigated analytically and numerically by using M-N interaction diagrams. A steel jacket comprising two C-sections connected to different numbers of welded batten plates was investigated. Finite element (FE) analysis was conducted using Abaqus/CAE software. The experimental data presented by Belal et al. [1] were used in this study. All columns had a cross-section of 200 × 200 mm with a height of 1200 mm and were reinforced with four longitudinal bars of 12 mm diameter with stirrups of 6 mm diameter every 125 mm. The first column was the reference column, which was not strengthened, whereas the other columns were strengthened using two C-sections with different numbers of connecting batten plates.

2. Literature Review

Belal et al. [1] investigated the behavior and failure load of strengthened RC columns using the steel jacket technique. Steel angles, C-sections, plates, and batten plates with a specific spacing were used as the strengthening systems. They used specimens with square cross-sections measuring 200 mm × 200 mm and a height of 1200 mm. The specimen without strengthening was used as a control. Their test results showed that using a steel jacket comprising four angles or two C-sections provided higher axial resistance than a steel jacket comprising four plates. In addition, increasing the number of steel battens in the four-angle steel jacket did not increase the axial resistance, unlike in the case of the two C-section steel jackets.

CEN 1994-1-1 Eurocode 4 [4] proposed an analytical model that enables the construction of M-N interaction diagrams for composite columns using the PSDM. This model does not include a direct application to RC columns reinforced with steel sections, nor does it consider the effects of confinement.

An easy hand-computation analytical model was developed by Al-Sherrawi & Salman [5] and Al-Haddad et al. [6] to build an interaction diagram for an RC column strengthened with a cage consisting of four steel angles and battens using the PSDM, and assuming that the strengthened RC column behaves as a composite column. This article provides numerous examples illustrating the use of these diagrams, which have been demonstrated to be straightforward and effective in both analytical and design applications.

An experimental program was presented by Abdelraheem et al. [8] which involved the use of ten rectangular RC columns strengthened with four steel angles and steel battens under an axial load. The primary research variables included the effect of the aspect ratio (from the long to the short side of the cross section), and the size and spacing of the steel battens. The columns were 200 × 200 mm, 160 × 250 mm, and 140 × 286 mm, with aspect ratios of 1, 1.56, and 2.04, and heights of 1200 mm, 960 mm, and 840 mm, respectively. Based on the results, the strengthening method was highly effective in enhancing the axial load capacity of the reinforced columns. This increase was attributed to the confining effect of the steel jacket and the ability of the steel angle to withstand a significant portion of the applied axial load. Buckling of the steel angles was the primary reason for failure in most of the strengthened samples.

Discrete steel plates can be welded horizontally (known as battens) or in an inclined direction (known as lacing). The use of battens and lacing significantly enhances the strength of RC columns. According to the numerical analysis conducted by Shhatha et al. [9], lacing with battens is the most effective pattern for using the same number of steel jackets with different cross-sectional areas. The study observed that, compared to battens alone the load-carrying capacity of the column increased by approximately 1.8% and 1.15% when the lacing angles were 60.832° and 74.407°, respectively, with the vertical axis of the column.

Erange et al. [10] proposed the use of steel jackets as a strengthening technique for RC columns. FE models of the strengthened columns were developed and validated using previous experimental data. Six groups of steel jacket sections with different batten spacings, batten thicknesses, batten widths, angle thicknesses, and steel jacket heights were tested under axial and lateral loads. An un-strengthened RC column was also analysed as a control specimen to compare its performance with that of the strengthened specimens. The study found that strengthening RC columns with steel jackets was effective in enhancing the lateral performance and resulted in a more stable load-displacement curve with lower strength degradation compared to the control specimen. The most effective method for increasing lateral strength and ductility is to increase the steel angle thickness. However, increasing the steel jacket height by up to 1/3rd of the RC column height also improved the lateral performance.

A new method to strengthen steel columns has been proposed by Shan et al. [11]. This method involves connecting steel plates using high-strength fasteners to form a steel-jacketed column. This new connection method was designed for quick and stable connections between two steel components. The procedure included five main steps: determining the lateral load capacity of the damaged RC columns, determining the spacing of the steel jacket connections, estimating the lateral load capacity of the strengthened RC columns, determining the axial load ratio of the strengthened RC columns, and determining the effective stiffness of the strengthened RC columns.

By assuming an equivalent stress block for concrete, Al-Sherrawi & Salman [12] and Fernandesa et al. [13] introduced two analytical models to create interaction diagrams for RC columns strengthened with steel jackets. The proposed model was consistent with the literature and showed good precision in estimating the ultimate moment values.

A nonlinear FE model has been proposed to simulate and study the behavior of a preloaded and non-damaged RC column after being strengthened with a steel jacket [14-16].

Shehab Eldeen et al. [17] presented a review that provided a thorough analysis of the techniques used to strengthen RC columns with steel jackets. This study included both experimental and analytical investigations to determine the impact on the load-carrying capacity, ductility, lateral strength, and flexural strength of parameters such as strip thickness, size and spacing, concrete strength, angle size, and thickness. The results of the experimental investigations were compared with analytical equations proposed by different researchers and design codes. The overall increase in axial strength ranged from 18.65% to 109%, and lateral strength from 63% to 68%. Reinforcing RC columns with steel jackets is an effective and reliable technique for improving their load-carrying capacities and overall strengths.

Villar-Salinas et al. [18] presented a study on the seismic performance of a six-storey RC building in Cartagena de Indias, Colombia. The building was retrofitted with steel jacketing to improve its ability to withstand seismic activity. This study investigated the influences of different material properties and load scenarios on the behavior of a building. The proposed steel jacketing increased the compressive and flexural capacities of the columns and improved the overall ductility of the building.

Based on plasticity rules and the non-linear behavior of materials, a proper constitutive law has been proposed by Minafò [19, 20] for modelling the interface between the concrete column surface and the steel jacket.

Abd-El-Nabil et al. [21] conducted a numerical study to investigate the effect of RC columns with steel jackets on their axial load capacity. The steel jacket comprised two C-sections connected to different numbers of welded batten plates. FE analysis was conducted using Abaqus/CAE software. The results of this study showed that using two C-sections as a steel jacket is highly effective because a relatively rigid jacket can increase the failure load of the columns by a minimum value of 21.46%. Additionally, the more batten plates connected to the two C-section steel jackets, the greater the confinement of the column, and hence, the greater the column failure load. Furthermore, connecting the two C-section steel jackets with a single large plate to form a complete box around the column provided the best confinement and could increase the failure of the column by 75.92%.

Salman & Al-Sherrawi [22] presented a method for constructing axial force-bending moment interaction diagrams for an RC and steel jacket columns. The focus was on an RC column strengthened with a steel jacket comprising vertical steel angles and horizontal steel battens. Two analytical methods have been used to construct the interaction diagrams: the strain compatibility method (SCM) and the PSDM. The SCM considers the position of the neutral axis on the stress of the concrete, reinforcing bars, and steel sections. In the PSDM, the position of the neutral axis did not affect the stress of the three components or the maximum value of the stress used for each component. The analytical results were compared with the experimental results for selected specimens and showed good agreement.

3. Analytical Model

This section introduces the process of constructing an M-N interaction diagram for an RC column strengthened with a steel jacket. The steel jacket consists of two vertical C-sections connected by horizontal battens. The placement of the C-section in (Figure 1) plays a significant role in determining the position of point D (see below). When an applied eccentric force causes a uniaxial bending moment about the major axis of a C-section, the four main points are as follows:

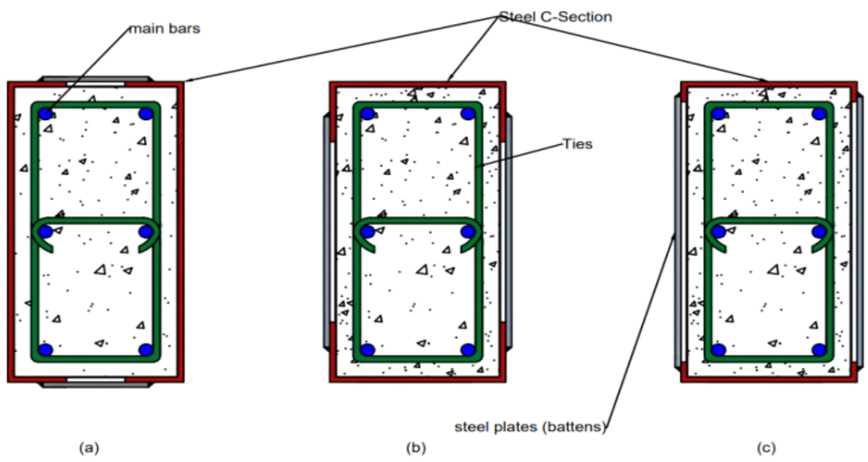

Figure 1. Types of steel jacket used

- Point A:

$$N_A = f_c\, bh + f_{ya}\, A_{ch} + f_{yr}\, A_{sr} + n_1 f_{yr}\, A_1,\ M_A = 0 \tag{1}$$

- Point C:

$$N_C = f_c \frac{h}{2} b \tag{2}$$

$$M_C = f_c \left[\frac{bh^2}{8}\right] + Z_{ch}\, f_{ya} + f_{yr}\, A_{sr}\left[d - \frac{h}{2}\right] \tag{3}$$

$$Z_{ch} = 4\left[\left[(b_1 - t_1)t_1\left(\frac{h+t_1}{2}\right)\right] + \frac{t_1 {h_1}^2}{8}\right] \tag{4}$$

- Point D was established as the flexural resistance of the composite section (M_D), whereas the axial resistance (N_D) was equal to zero. The location of the neutral axis (c) was assumed and verified. c was determined by applying $\sum F = N_D$ and using $N_D = 0$. Possible assumptions may be studied to determine c, depending on the relationship between the bending and the major axis of the C-sections (see Table 1 to 3).

Table 1. Possible assumptions for the position of *c* at point D when the bending is about the major axis of the C-sections

$\left(\frac{h}{2} - \frac{d_1}{2}\right) < c < \frac{h}{2}$	
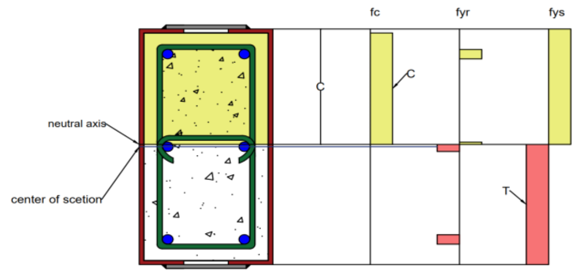	$c = \frac{2\, t_1 f_{ya} h + (A_1 - 2A_i) n_1 f_{yr}}{f_c\, b + 4 f_{ya}\, t_1},\ A_i = d_1 h_i,\ h_i = c - \frac{h}{2} + \frac{d_1}{2}$ $M_D = f_c\, bc\left(\frac{h}{2} - \frac{c}{2}\right) + Z_{ch} f_{ya} - \left[4t_1\left(\frac{h}{2} - c\right) f_{ya}\left(\frac{h}{2} - c - \left(\frac{\frac{h}{2} - c}{2}\right)\right)\right] +$ $n_1 A_i f_{yr}\left(\frac{d_1}{2} - c\frac{h_i}{2}\right) - \left[(A_1 - A_i) n_1 f_{yr}\left(\frac{d_1}{2} - \left(\frac{d_1 - h_i}{2}\right)\right)\right] + A_{sr}\, f_{yr}\left(\frac{h}{2} - d'\right)$
$0 < c \leq \left(\frac{h}{2} - \frac{d_1}{2}\right)$	
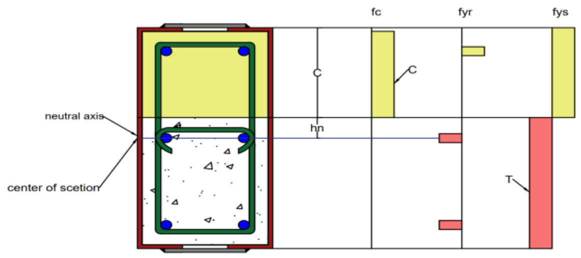	$c = \frac{2\, t_1 f_{ya} h + n_1 A_1 f_{yr}}{f_c\, b + 4 f_{ya}\, t_1}$ $M_D = f_c\, bc\left(\frac{h}{2} - \frac{c}{2}\right) + Z_{ch}\, f_{ya} - \left[4t_1\left(\frac{h}{2} - c\right) f_{ya}\left(\frac{h}{2} - c - \left(\frac{\frac{h}{2} - c}{2}\right)\right)\right] +$ $A_{sr}\, f_{yr}\left(\frac{h}{2} - d'\right)$
$\left(d' - \frac{d_{bar}}{2}\right) < c < \left(d' + \frac{d_{bar}}{2}\right)$	
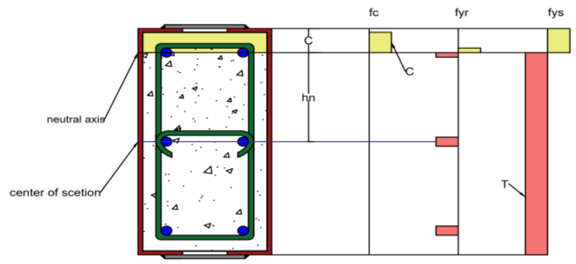	$c = \frac{2\, t_1 f_{ya} h + (A_{sr} + n_1 A_1 - n A_i) f_{yr}}{f_c\, b + 4 f_{ya}\, t_1},\ A_i = d_{bar} h_i,\ h_i = c - concrete\ cover - d_{tie}$ $M_D = f_c\, bc\left(\frac{h}{2} - \frac{c}{2}\right) + Z_{ch}\, f_{ya} - \left[4t_1\left(\frac{h}{2} - c\right) f_{ya}\left(\frac{h}{2} - c - \left(\frac{\frac{h}{2} - c}{2}\right)\right)\right] +$ $\frac{n}{2} A_i f_{yr}\left(\frac{h}{2} - c + \frac{h_i}{2}\right) - \left[\left(\frac{A_{sr}}{2} - \frac{n}{2} A_i\right) f_{yr}\left(\frac{h}{2} - c - \left(\frac{d_{bar} - h_i}{2}\right)\right)\right] + \frac{A_{sr}}{2}\, f_{yr}\left(\frac{h}{2} - d'\right)$
$0 < c \leq \left(d' - \frac{d_{bar}}{2}\right)$	
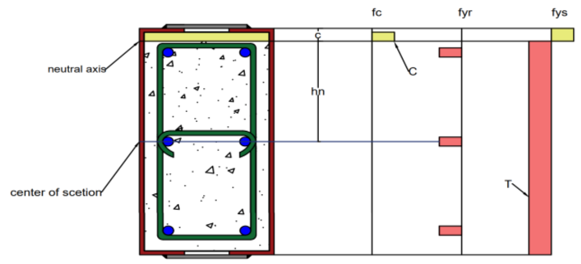	$c = \frac{2\, t_1 f_{ya} h + (A_{sr} + n_1 A_1)\, f_{yr}}{f_c b + 4 f_{ya}\, t_1}$ $M_D = f_c\, bc\left(\frac{h}{2} - \frac{c}{2}\right) + Z_{ch}\, f_{ya} - \left[4t_1\left(\frac{h}{2} - c\right) f_{ych}\left(\frac{h}{2} - c - \left(\frac{\frac{h}{2} - c}{2}\right)\right)\right]$

Table 2. Possible assumptions for the position of *c* at point D for case I when the bending is about the minor axis of the C-sections

$$\left(\frac{h}{2}-\frac{d_1}{2}\right) < c < \frac{h}{2}$$

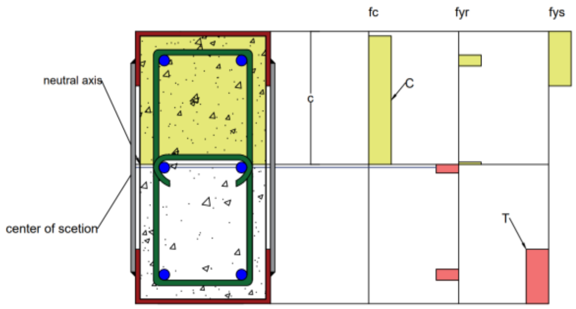

$$c = \frac{(A_1-2A_i)n_1 fyr}{f_c\, b};\ A_i = d_1 h_i\ ;\ h_i = c - \frac{h}{2} + \frac{d_1}{2}$$

$$M_D = f_c\, bc\left(\frac{h}{2}-\frac{c}{2}\right) + Z_{ch}\, f_{ya} + n_1 A_i f_{yr}\ \left(\frac{d_1}{2} - c\,\frac{h_i}{2}\right) - \left[(A_1 - A_i)n_1 f_{yr}\left(\frac{d_1}{2} - \left(\frac{d_1-h_i}{2}\right)\right)\right] + A_{sr}\, f_{yr}\ \left(\frac{h}{2} - d'\right)$$

$$(b_1 - t_1) \le c \le \left(\frac{h}{2}-\frac{d_1}{2}\right)$$

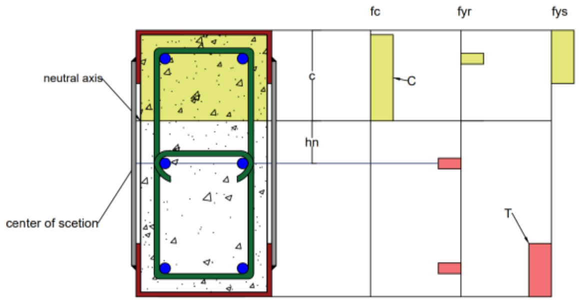

$$c = \frac{n_1 A_1 fyr}{f_c\, b}$$

$$M_D = f_c bc\left(\frac{h}{2}-\frac{c}{2}\right) + Z_{ch}\, f_{ya} + A_{sr}\, f_{yr}\ \left(\frac{h}{2} - d'\right)$$

$$0 < c\ < (b_1 - t_1)\ \ and\ c \ge \left(d' + \frac{d_{bar}}{2}\right)$$

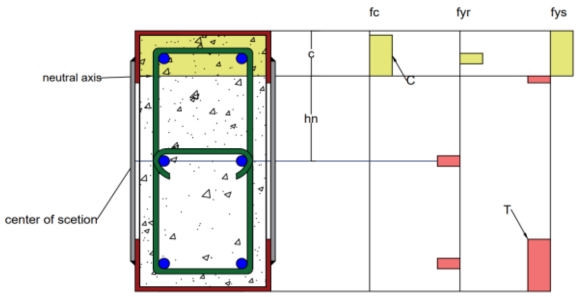

$$c = \frac{4t_1 fya(b_1-t_1)+n_1 A_1 fyr}{f_c\, b + 4t_1 fya}$$

$$M_D = f_c\, bc\left(\frac{h}{2}-\frac{c}{2}\right) + Z_{ch}\, f_{ya} + A_{sr}\, f_{yr}\ \left(\frac{h}{2} - d'\right) - \left[4t_1(b_1 - t_1 - c)f_{ya}\left(\frac{h}{2} - c - \left(\frac{b_1-t_1-c}{2}\right)\right)\right]$$

$$0 < c\ < (b_1 - t_1)\ and\ \left(d' - \frac{d_{bar}}{2}\right) < c < \left(d' + \frac{d_{bar}}{2}\right)$$

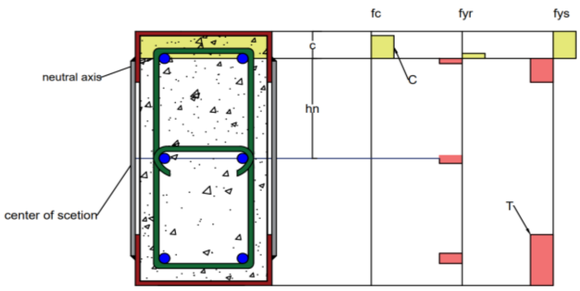

$$c = \frac{4t_1(b_1-t_1)f_{ya} + (A_{sr}+n_1 A_1 - nA_i)f_{yr}}{f_c\, b + 4\, t_1 f_{ya}},\ A_i = d_{bar} h_i,\ h_i = c - concrete\ cover - d_{tie}$$

$$M_D = f_c\, bc\left(\frac{h}{2}-\frac{c}{2}\right) + Z_{ch}\, f_{ya} - \left[4t_1(b_1 - t_1 - c)f_{ya}\left(\frac{h}{2} - c - \left(\frac{b_1-t_1-c}{2}\right)\right)\right] + \frac{n}{2}A_i f_{yr}\ \left(\frac{h}{2} - c + \frac{h_i}{2}\right) - \left[\left(\frac{A_{sr}}{2} - \frac{n}{2}A_i\right) f_{yr}\left(\frac{h}{2} - c - \left(\frac{d_{bar}-h_i}{2}\right)\right)\right] + \frac{A_{sr}}{2}\ f_{yr}\ \left(\frac{h}{2} - d'\right)$$

$$0 < c\ < (b_1 - t_1)\ and\ c \le \left(d' - \frac{d_{bar}}{2}\right)$$

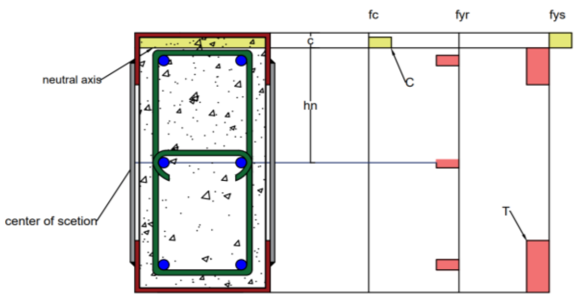

$$c = \frac{4t(b_1-t_1)f_{ya} + (A_{sr}+n_1 A_1)\, f_{yr}}{f_c b + 4 f_{ya}\, t_1}$$

$$M_D = f_c\, bc\left(\frac{h}{2}-\frac{c}{2}\right) + Z_{ch} f_{ya} - \left[4t_1(b_1 - t_1 - c)f_{ya}\left(\frac{h}{2} - c - \left(\frac{b_1-t_1-c}{2}\right)\right)\right]$$

Table 3. Possible assumptions for the position of c at point D for case II when the bending is about the minor axis of the C-sections

$$\left(\frac{h}{2}-\frac{d_1}{2}\right) < c < \frac{h}{2}$$

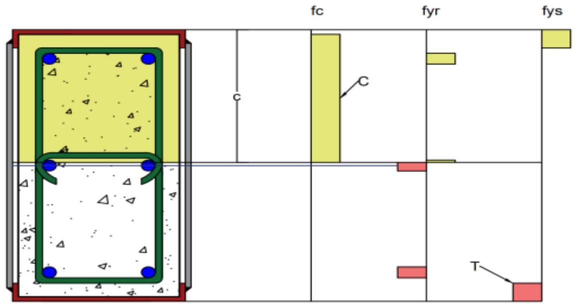

$$c = \frac{(A_1-2A_i)n_1 f_{yr}}{f_c\, b}\ ;\ A_i = d_1 h_i\ ;\ h_i = c-\frac{h}{2}+\frac{d_1}{2}$$

$$M_D = f_c\, bc\left(\frac{h}{2}-\frac{c}{2}\right)+Z_{ch}\, f_{ya}+n_1 A_i f_{yr}\ \left(\frac{d_1}{2}-c\,\frac{h_i}{2}\right)-\left[(A_1-A_i)n_1 f_{yr}\left(\frac{d_1}{2}-\left(\frac{d_1-h_i}{2}\right)\right)\right]+A_{sr}\, f_{yr}\ \left(\frac{h}{2}-d'\right)$$

$$\left(d'+\frac{d_{bar}}{2}\right) \le c \le \left(\frac{h}{2}-\frac{d_1}{2}\right)$$

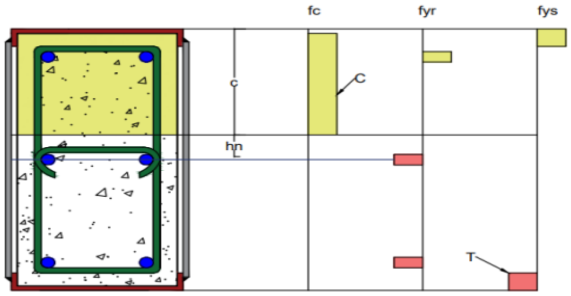

$$c = \frac{n_1 A_1 f_{yr}}{f_c\, b}$$

$$M_D = f_c\, bc\left(\frac{h}{2}-\frac{c}{2}\right)+Z_{ch}\, f_{ya}+A_{sr}\, f_{yr}\ \left(\frac{h}{2}-d'\right)$$

$$\left(d'-\frac{d_{bar}}{2}\right) < c < \left(d'+\frac{d_{bar}}{2}\right)$$

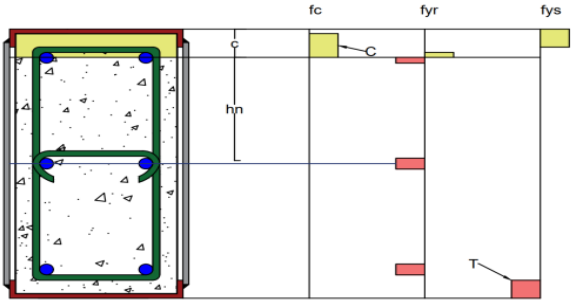

$$c = \frac{(A_{sr}+n_1 A_1-nA_i)f_{yr}}{f_c\, b}\ ,\ A_i = d_{bar}h_i, h_i = c - concrete\ cover - d_{tie}$$

$$M_D = f_c\, bc\left(\frac{h}{2}-\frac{c}{2}\right)+Z_{ch}\, f_{ya}+\frac{n}{2}A_i f_{yr}\ \left(\frac{h}{2}-c+\frac{h_i}{2}\right)-\left[\left(\frac{A_{sr}}{2}-\frac{n}{2}A_i\right)f_{yr}\left(\frac{h}{2}-c-\left(\frac{d_{bar}-h_i}{2}\right)\right)\right]+\frac{A_{sr}}{2}\ f_{yr}\ \left(\frac{h}{2}-d'\right)$$

$$(b_1-t) \le c\ \le \left(d'-\frac{d_{bar}}{2}\right)$$

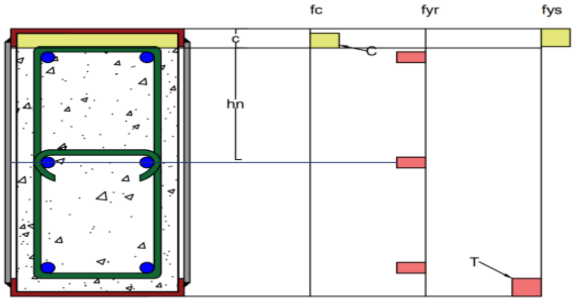

$$c = \frac{(A_{sr}+n_1 A_1)\, f_{yr}}{f_c\, b}$$

$$M_D = f_c\, bc\left(\frac{h}{2}-\frac{c}{2}\right)+Z_{ch}\, f_{ya}$$

$$0 < c\ < (b_1-t)$$

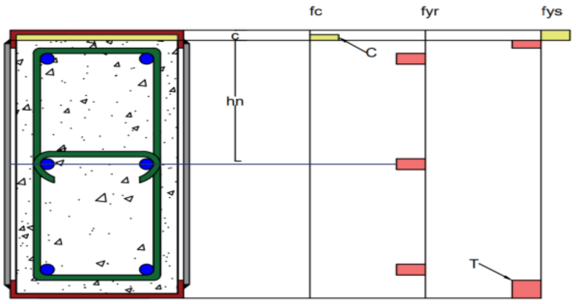

$$c = \frac{4t_1(b_1-t_1)f_{ya}+(A_{sr}+n_1 A_1)\, f_{yr}}{f_c b+4f_{ya}\, t_1}$$

$$M_D = f_c\, bc\left(\frac{h}{2}-\frac{c}{2}\right)+Z_{ch}\, f_{ya}-\left[4t_1(b_1-t_1-c)f_{ya}\left(\frac{h}{2}-c-\left(\frac{b_1-t_1-c}{2}\right)\right)\right]$$

- Point B matches the plastic neutral axis position which produces the same flexural resistance as point D, with twice the axial resistance of point C.

$$N_B = 2N_C$$
$$M_B = M_D$$

When the applied eccentric force causes a uniaxial bending moment about the minor axis of the C-sections, two possible cases can be observed depending on whether the leg length of the C-section on the compression side exceeds the position of the compression reinforcement and changes in the calculation of Z_{ch} for point C, as explained below:

$$Z_{ch} = 4\left[\left[(h_1 - 2t_1)t_1\left(\frac{h+t_1}{2}\right)\right] + \left[b_1 t_1\left(\frac{h}{2} + t_1 - \frac{b_1}{2}\right)\right]\right] \tag{5}$$

Point D is the flexural resistance of the composite section (M_D), whereas the axial resistance (N_D) is zero (the eccentricity equals infinity). The location of the neutral axis *c* must be assumed and adjusted later. c can be determined by applying $\sum F = N_D$ and using $N_D = 0$, Possible assumptions may be made to determine *c* as listed in Tables 2 and 3. A simple flowchart is shown in (Figure 2) for simplicity and better understanding.

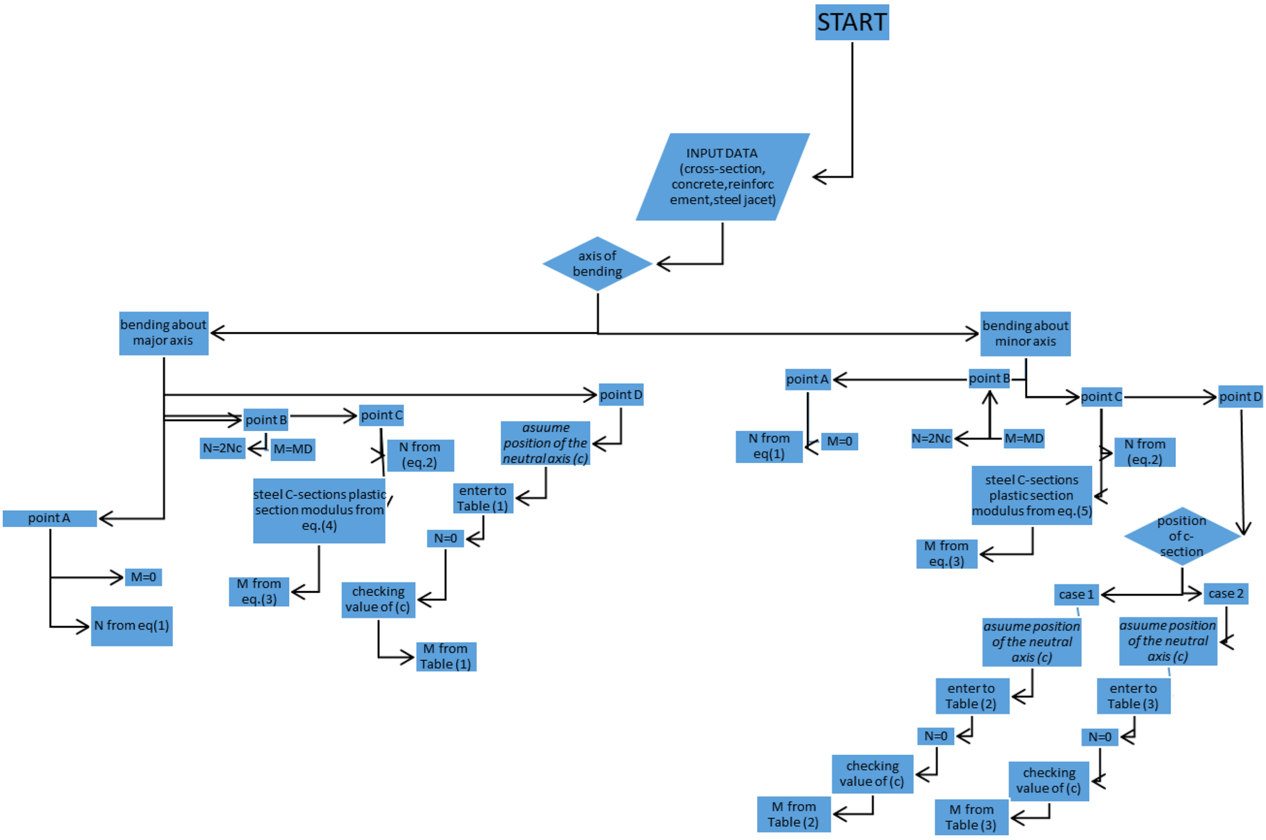

Figure 2. Simple flowchart for finding the points of interaction diagram

4. FE Model

The ABAQUS v.6.13 [2] software was used to model the FE model. The material nonlinearity of the concrete, reinforcement, and steel jacket, second-order geometric effects, and the existence of the column-steel jacket interface were considered to accurately simulate the behavior of the strengthened RC column [15, 16, 23].

The two experimental specimens shown in (Figure 3) tested by Belal et al. [1] were analysed to validate the analytical and FE models. The details of the specimens are listed in Table 4. The analytical and FE results are discussed in this section. These results were compared with the experimental results.

Table 4. Details of specimens used

Specimen	Cross-section (mm)	Length (mm)	Longitudinal bars (mm)	Tie (mm)	Steel section dimensions (mm)	Steel strip dimensions (mm)	Clear strip spacing (mm)	f_c (MPa)	f_{yr} (MPa)	f_{yan} (MPa)	f_{yst} (MPa)
Col.03.C.3P	200 × 200	1200	4 φ 12	Φ 6 @ 125 mm	2 C 206 ×50 × 3.1	150 × 100 × 5	440	27.2	360	360	360
Col.04.C.6P	200 × 200	1200	4 φ 12	Φ 6 @ 125 mm	2 C 206 ×50 × 3.1	150 × 50 × 5	190	27.2	360	360	360

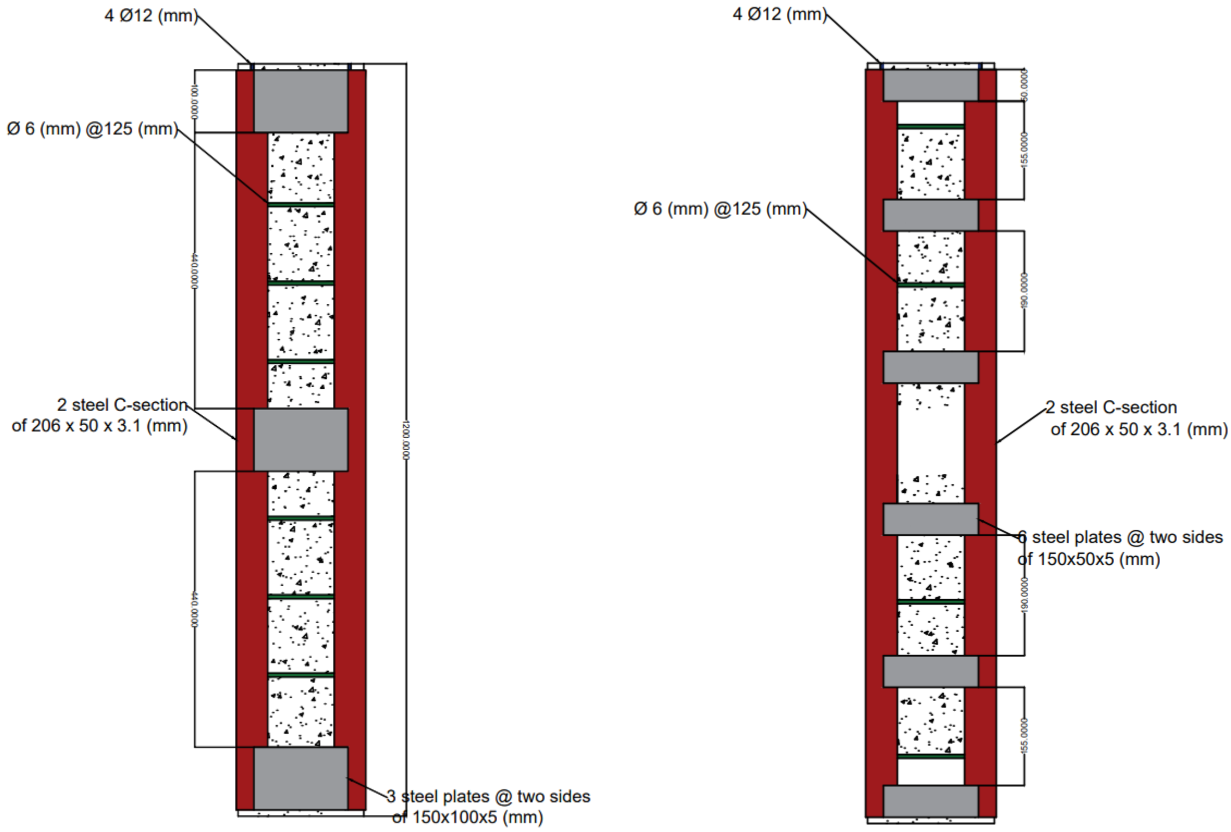

Figure 3. Specimen dimensions and steel jacket configuration [1]

To validate the FE model used in this study, the FE results were compared with the experimental results presented by Belal et al. [1] and the FE results of a strengthened RC column tested by Abd-El-Nabil et al. [21]. The load-displacement curves were plotted for the experimental and FE models and compared, as shown in Figure 4, and showed good agreement between the experimental and modelled columns.

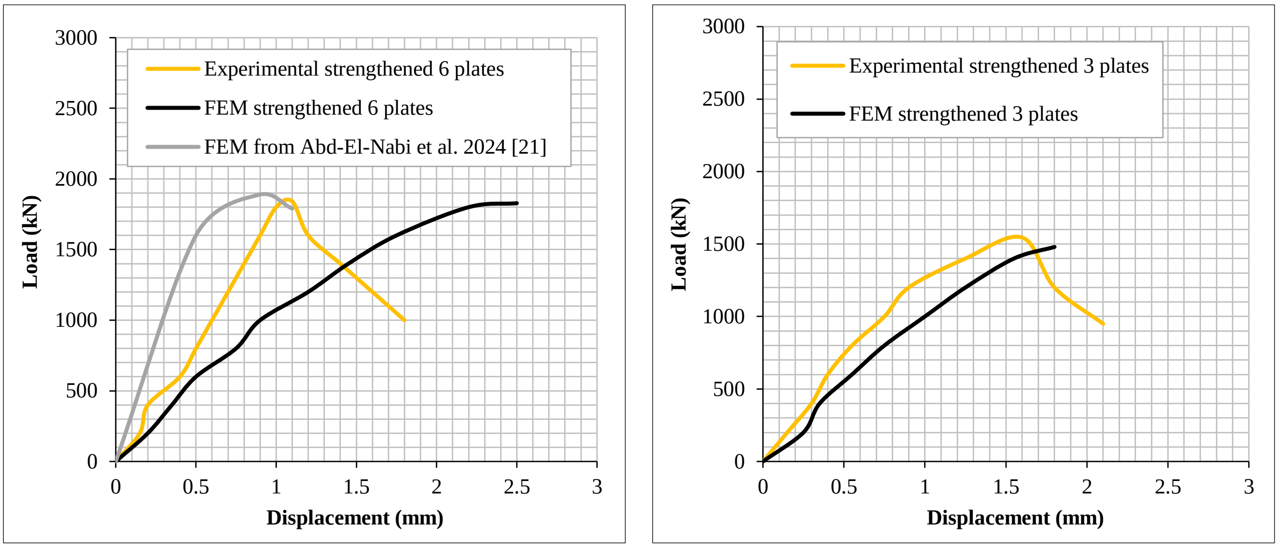

Figure 4. The load-displacement curve of the experimental results: (a) Col.03.C.3P, (b) Col.04.C.6P

Table 5 summarises the increase of the failure load for the strengthened column for the analytical and FE models. For Col.03.C.3P the increase percentages of the failure load were 292.6% and 133.3% while for Col.04.C.6P the steel cage is more effective due to adding more batten plates to connect the two C-sections, which provides more confinement to the column hence increasing the failure load significantly. The analytical model predicts more improvement than the FE model due to the assumption of yielding of all reinforcing bars and the steel jacket without considering the position of the neutral axis.

Table 5. The improvement in axial and flexural resistance

Specimen	Analytical model				FE model			
	Major axis		Minor axis		Major axis		Minor axis	
	%M	%N	%M	%N	%M	%N	%M	%N
Col.03.C.3P	472.6	76.47	411.11	76.47	292.6	36	133.3	36
Col.04.C.6P	472.6	76.47	411.11	76.47	308.8	68	263.7	68

As the load increased, cracks started to appear in the upper and lower thirds of the column and increased until total collapse. In addition, local failure in the two C-sections began to appear in the upper and lower thirds when the load approached the failure load. The confinement provided by the steel cage increased the column failure load to 1828 kN and 1480 kN, with a corresponding displacement of 2.5 mm and 1.8 mm for the sixth and third connecting batten plates, respectively. The steel cage was more effective, and the failure load increased significantly. Different failure modes of the strengthened RC columns were observed owing to the effects of eccentricity, as shown in Figures 5 to 9.

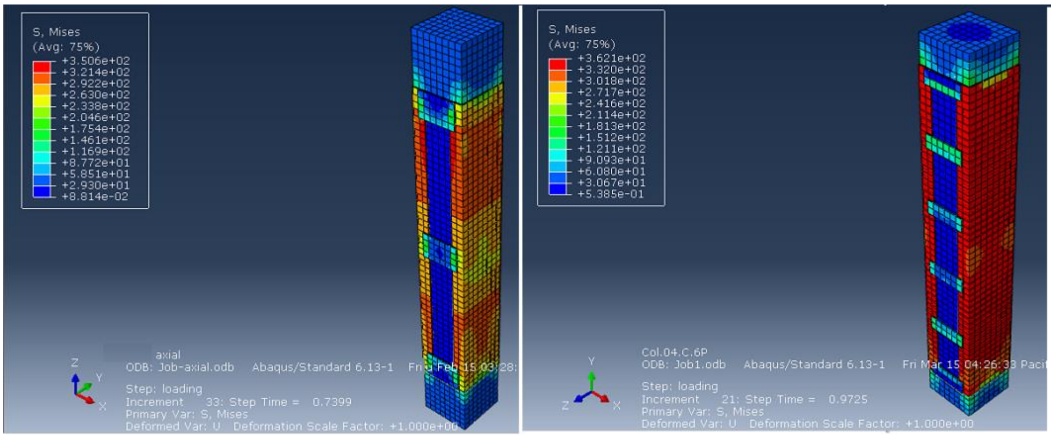

Figure 5. Strengthened RC model under concentric axial force

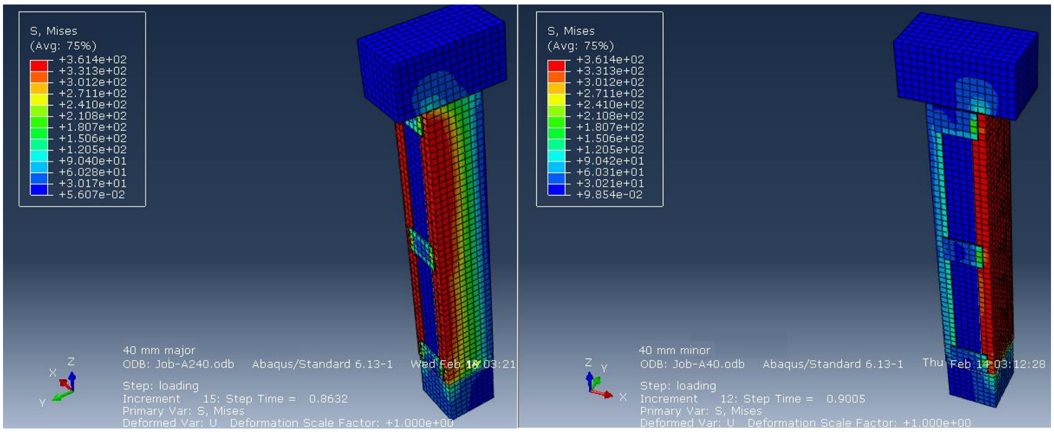

Figure 6. Col.03.C.3P under axial force with eccentricity of 40 mm about the major and the minor axis

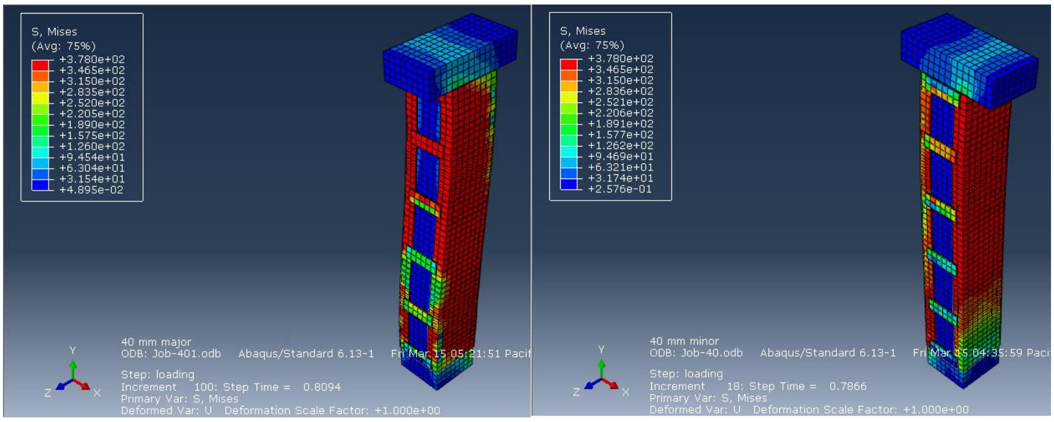

Figure 7. Col.04.C.6P under axial force with eccentricity of 40 mm about the major and the minor axis

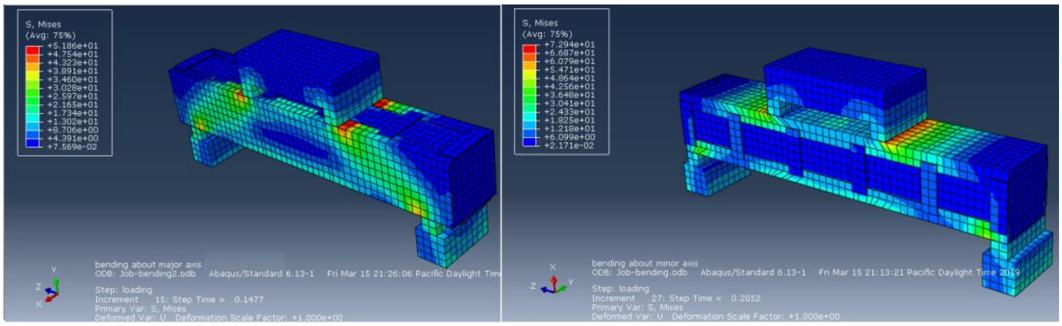

Figure 8. Col.04.C.6P under pure bending moment about the major and the minor axis

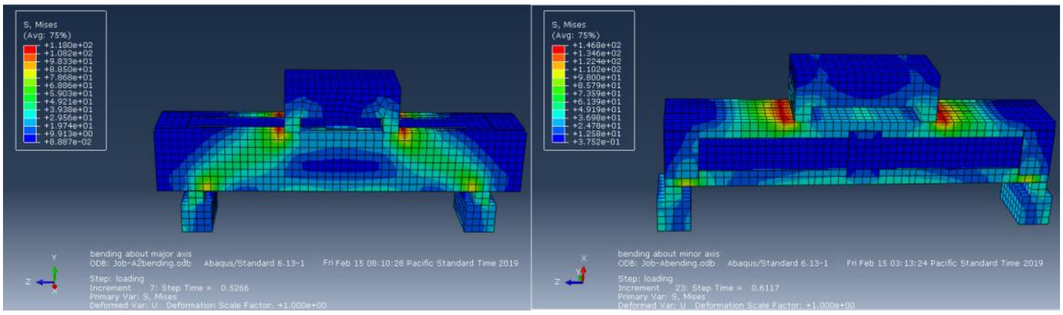

Figure 9. Col.03.C.3P under pure bending moment about the major and the minor axis

When the strengthened RC column model was subjected to an axial force with a specified eccentricity, cracks began to initiate on the tension side of the strengthened column. The steel (reinforcing bars and steel section) on that side is in tension, and the stress depends on the eccentricity. For a small amount of eccentricity, the stresses were observed to be below the yield value, whereas for a further increase in eccentricity as shown in Figures 6 and 7, the steel on the tensile side reaches its yield stress before concrete crushing. The strengthened RC column behaves as a beam until it reaches an eccentricity of infinity (pure bending), as shown in Figures 8 and 9.

Figures 10 to12 show that bending about the minor axis yields higher flexural values than about the major axis owing to the plastic section modules for the C-section. Increasing the number of battens increases the axial and flexural strengths of the strengthened RC column owing to the increase in confinement, unlike the analytical method, in which there is no effect of battens on the axial and flexural resistance. The experimental specimen results were considered safe when compared to the M-N values obtained.

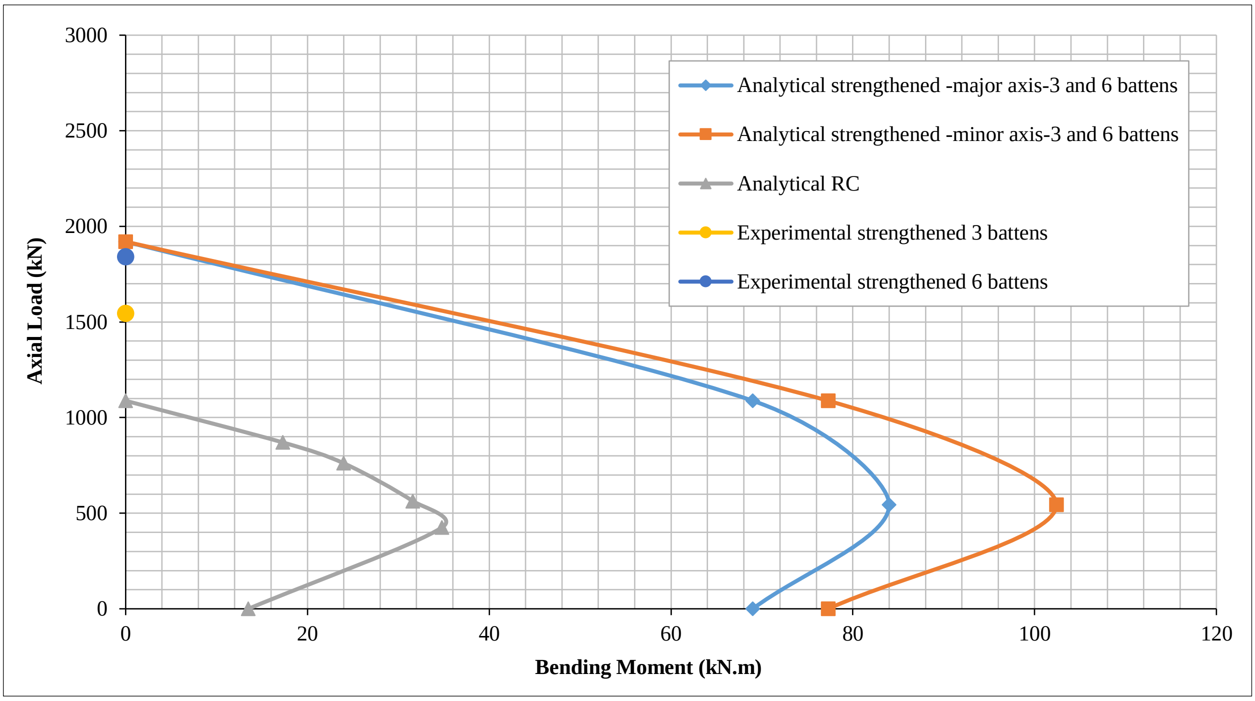

Figure 10. Experimental and analytical results for Col.03.C.3P and Col.04.C.6P specimen

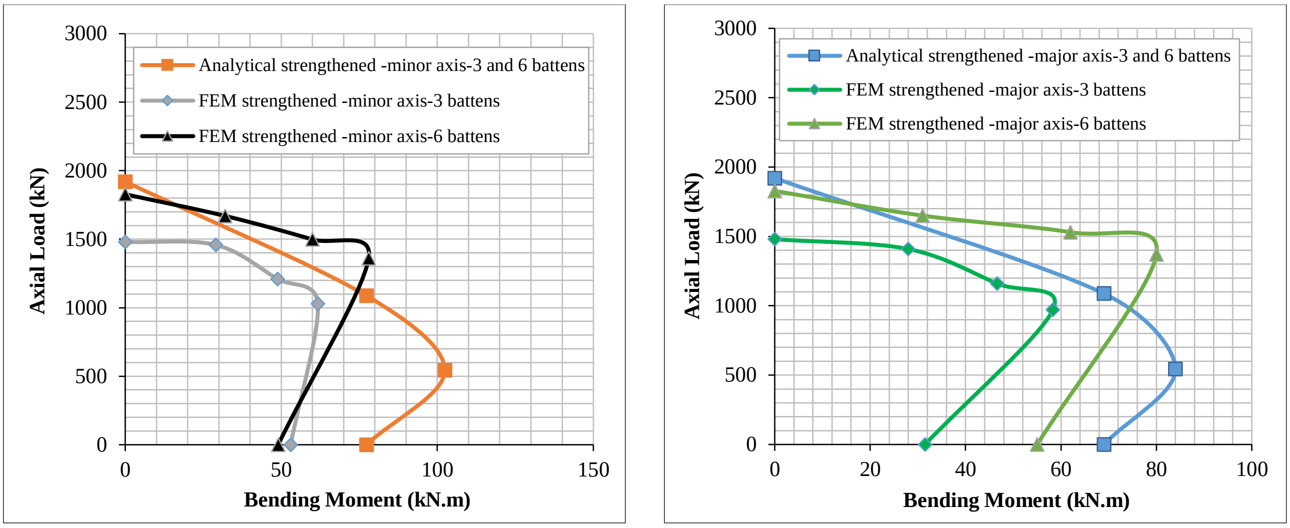

Figure 11. Analytical and FE results for Col.03.C.3P and Col.04.C.6P specimens about the minor and major axis, respectively

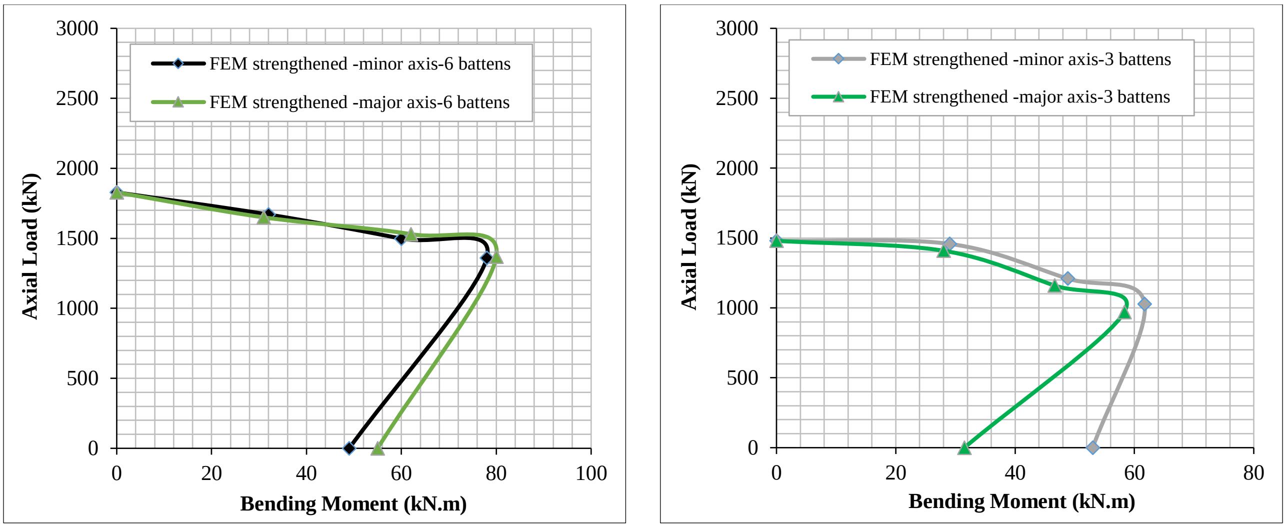

Figure 12. FE results for each specimen about the major and minor axis

5. Conclusions

Based on the numerical simulation and analysis of the results, the following conclusions were drawn:

- Using two C-section steel jackets can increase the failure load of columns owing to their relatively rigid structures.
- The use of two C-section steel jackets enhanced the ductility of the RC columns. The greater the number of batten plates connecting the two C-section steel jackets, the greater the confinement of the column, and hence, the greater the increase in the column failure load.
- The Abaqus/CAE software simulation of the RC strengthened columns was acceptable because the failure loads and displacements closely matched those of the tested columns found in the literature.
- When the number of steel battens increases, the FE model provides higher axial and flexural resistances than the PSDM, especially in the compression failure zone, owing to the increase in confinement, which is neglected in the PSDM.

6. Nomenclature

fc	Cylinder compressive strength	*fyr*	Yield strength of reinforcement
fya	Yield strength of steel C-sections	*b*	Column width
h	Column height	*d*	Column effective depth
b1	Length of C-section leg	*h1*	Height of C-section

t1	Thickness of C-section	*Ach*	Total area of steel C-sections
Asr	Total area of corner reinforcement	*A1*	Area of central reinforcing bars
n1	Number of central reinforcing bars	*Zch*	Steel C-sections plastic section modulus
dbar	Diameter of longitudinal reinforcing bars	*d'*	Upper reinforcement effective depth
hi	Height of the part of central reinforcing bars under compression	*d1*	Diameter of central reinforcing bars
c	Position of the neutral axis	*Ai*	Area of the central reinforcing bars under compression
dtie	Diameter of tie reinforcing bars	*N*	Total number of reinforcing bars
NA	Axial load resistance at point A	*NB*	Axial load resistance at point B
NC	Axial load resistance at point C	*ND*	Axial load resistance at point D
MA	Flexural resistance at point A	*MB*	Flexural resistance at point B
MC	Flexural resistance at point C	*MD*	Flexural resistance at point D

7. Declarations

7.1. Author Contributions

Conceptualization, A.M.; methodology, S.H.; software, S.H.; validation, S.H.; formal analysis, S.S.; investigation, A.M.; resources, A.M.; data curation, S.H.; writing—original draft preparation, A.M.; writing—review and editing, A.M.; visualization, S.H.; supervision, A.M.; project administration, A.M.; funding acquisition, S.H. All authors have read and agreed to the published version of the manuscript.

7.2. Data Availability Statement

The data presented in this study are available on request from the corresponding author.

7.3. Funding

The authors received no financial support for the research, authorship, and/or publication of this article.

7.4. Conflicts of Interest

The authors declare no conflict of interest.

8. References

[1] Belal, M. F., Mohamed, H. M., & Morad, S. A. (2015). Behavior of reinforced concrete columns strengthened by steel jacket. HBRC Journal, 11(2), 201–212. doi:10.1016/j.hbrcj.2014.05.002.

[2] Malavisi, M., Di Trapani, F., Marano, G. C., & Greco, R. (2019). Optimal seismic retrofitting of reinforced concrete columns with steel jacketing technique: a pushover-based genetic algorithm approach. Atti del XVIII Convegno ANIDIS L'ingegneria Sismica in Italia: Ascoli Piceno, 15-19 September, 2019, Ascoli Piceno, Italy.

[3] Charles G.. Salmon, & John E.. Johnson. (1996). Steel Structures: Design and Behavior. HarperCollins College, New York, United States.

[4] CEN 1994-1-1. (2004). Design of composite steel and concrete structures. Part 1: general rules and rules for buildings. European Committee for Standardization (CEN), Brussels, Belgium.

[5] Al-Sherrawi, M. H., & Salman, H. M. (2017). Analytical model for construction of interaction diagram for RC columns strengthened by steel jacket. International Journal of Science and Research, 6(10), 324-328.

[6] Al-Haddad, S. A., Fattah, M. Y., & Al-Sherrawi, M. H. (2024). Dimensionless interaction diagrams for reinforced concrete columns strengthened with steel angles and strips. AIP Conference Proceedings, 2864, 050007. doi:10.1063/5.0186732.

[7] Ahmed, B., Zerfu, K., & Agon, E. C. (2021). Construction of Uniaxial Interaction Diagram for Slender Reinforced Concrete Column Based on Nonlinear Finite Element Analysis. Advances in Civil Engineering, 2021, 1–10. doi:10.1155/2021/3275512.

[8] Abdelraheem, H., Ahmed, A. R. M., Ahmed, M. M., & Haridy, A. E. K. (2023). Behavior of RC Columns Strengthened with Steel Jacket Under Static Axial Load. Journal of Engineering Sciences, 51(2), 93-108.

[9] Shhatha, M. A., Mahdi, W. H., & Alalikhan, A. A. (2023). Assessment for behavior of axially loaded reinforced concrete columns strengthened by different patterns of steel-framed jacket. Open Engineering, 13(1), 20220414. doi:10.1515/eng-2022-0414.

[10] Erange, Y. G. P., Jenothan, M., Jayasinghe, J. A. S. C., Bandara, C. S., & Dammika, A. J. (2023). Enhancement of the Lateral Performance of RC Columns Using Steel Jacketing: A Numerical Approach. Engineer: Journal of the Institution of Engineers, Sri Lanka, 56(2), 51–64. doi:10.4038/engineer.v56i2.7576.

[11] Shan, Z., Chen, L., Liang, K., Su, R. K. L., & Xu, Z. D. (2021). Strengthening design of RC columns with direct fastening steel jackets. Applied Sciences, 11(8), 3649. doi:10.3390/app11083649.

[12] Al-Sherrawi, M. H., & Salman, H. M. (2017). Construction of N-M Interaction Diagram for Reinforced Concrete Columns Strengthened with Steel Jackets Using Plastic Stress Distribution Method. Civil Engineering Journal, 3(10), 929. doi:10.28991/cej-030926.

[13] Fernandes, M., De Nardin, S., & de Almeida Filho, F. M. (2022). M-N interaction curves for rectangular concrete-filled steel tube columns subjected to uniaxial bending moments. Revista IBRACON de Estruturas e Materiais, 15(1), e15108. doi:10.1590/S1983-41952022000100008.

[14] Esmaeilnia Omran, M., & Mollaei, S. (2017). Investigation of Axial Strengthened Reinforced Concrete Columns under Lateral Blast Loading. Shock and Vibration, 2017, 1–18. doi:10.1155/2017/3252543.

[15] Handhal, M. M., Abdulghani, A. W., & Al-Haydary, M. M. (2023). Structural Behavior of Steel Reinforced Concrete Joint Under Flexural Loads. Civil Engineering Journal, 9(3), 714-730. doi:10.28991/CEJ-2023-09-03-015.

[16] Shallan, O., Sakr, T., Khater, M., & Ismail, A. (2022). Interaction diagram for RC column strengthened by steel angles and strips. Frattura Ed Integrita Strutturale, 16(60), 1–12. doi:10.3221/IGF-ESIS.60.01.

[17] Eldeen, M. H. M. S., Hassan, M. H. A., & Salah, M. G. (2021) Strengthening of Reinforced Concrete Long Rectangular Columns by Steel. Research Paper on Concrete Structures, Menoufia University- Reinforced Concrete Research Group, 1-8.

[18] Villar-Salinas, S., Guzmán, A., & Carrillo, J. (2021). Performance evaluation of structures with reinforced concrete columns retrofitted with steel jacketing. Journal of Building Engineering, 33, 101510. doi:10.1016/j.jobe.2020.101510.

[19] Minafò, G. (2019). Analytical modelling of force transmission in axially loaded RC columns with indirectly loaded jackets. Engineering Structures, 181, 15–26. doi:10.1016/j.engstruct.2018.12.004.

[20] Minafò, G. (2019). An interface model for the analysis of the compressive behavior of RC columns strengthened by steel jackets. Structural Engineering and Mechanics, 71(3), 233–244. doi:10.12989/sem.2019.71.3.233.

[21] Abd-El-Nabi, E., Zahran, F., & Selouma, T. (2024). Numerical Analysis of Reinforced Concrete Columns Strengthened with Steel Jacket. Fayoum University Journal of Engineering, 7(2), 21–30. doi:10.21608/fuje.2024.343760.

[22] Salman, H. M., & Al-Sherrawi, M. H. (2018). Interaction diagram for a reinforced concrete column strengthened with steel jacket. International Journal of Civil Engineering and Technology, 9(6), 1369–1377.

[23] Zhu, T., Liang, H., Lu, Y., Li, W., & Zhang, H. (2020). Axial behavior of slender concrete-filled steel tube square columns strengthened with square concrete-filled steel tube jackets. Advances in Structural Engineering, 23(6), 1074-1086. doi:10.1177/1369433219888726.